are shown in Fig. 6. Note that nearly the same trend (to within experimental error) is observed for both powdered and block shale samples. Apparently, the degradation process is nearly independent of particle size.

To confirm that this agreement was not just fortuitous, we measured the effects of slow heating conditions (2°C/hr) on material 3.2-, 7.2-, and 11.8-cm diam. To within experimental error, all particle sizes gave the same yield. A summary of yield data from the these experiments is given in Table 2 and 3.

During previous experiments[5] on powder shale samples, we observed similar oil degradation (i.e., yield loss) from prolonged isothermal heating under autogenous conditions. However, sweeping

TABLE 3.
Summary of Oil Shale Powder Experiments (22 gal/ton Material[a] under Linear Heating Conditions, i.e., dT/dt = Const).

Sample No.	Heating rate, °C/hr	External flow[b] rate, cm^3/min	Oil yield % FA
RP-1	0.6	0	78.8
TC-22	5.0	0	86.1
TC-18	5.0	0	85.7
TC-20	19.3	0	90.8
TC-14	63.5	0	96.1
TC-12	185.0	0	98.4
Fischer Assay	720	0	100.0
TC-28	5	2.0	86.7
TC-52	5	5.2	89.8
TC-34	5	7.0	91.9
TC-56	5	15.0	92.9
TC-38	5	18.6	97.4
TC-48[c]	19.3	0	91.0

[a] 9.914 wt% organic carbon in raw shale.

[b] A zero flow indicates autogenous conditions.

[c] Retort vessel inverted.

(to within
block shale
y

tous, we
r) on
rimental
ary of
e 2 and 3.
es, we
om prolonged
ver, sweeping

the sample with an inert gas reduced the yield loss, since the liberated oil was removed from the pyrolysis region before being degraded.

The ability of a sweep gas to reduce oil degradation was also observed in the nonisothermal (linear heating rate) powder experiments. Powdered shale samples heated at 5°C/hr showed a near linear increase in yield with low gas sweep rate (<18cm^3/min — i.e. < 1 retort void volume/min.) — see Table 3 and Fig. 7. Hence, the effects of gas sweep rate and heating rate closely parallel each other.

These results indicate that a higher heating rate may allow the recovery of more oil in both powders and blocks because it

Material[a]
nst).

il yield % FA
78.8
86.1
85.7
90.8
96.1
98.4
100.0
86.7
89.8
91.9
92.9
97.4
91.0

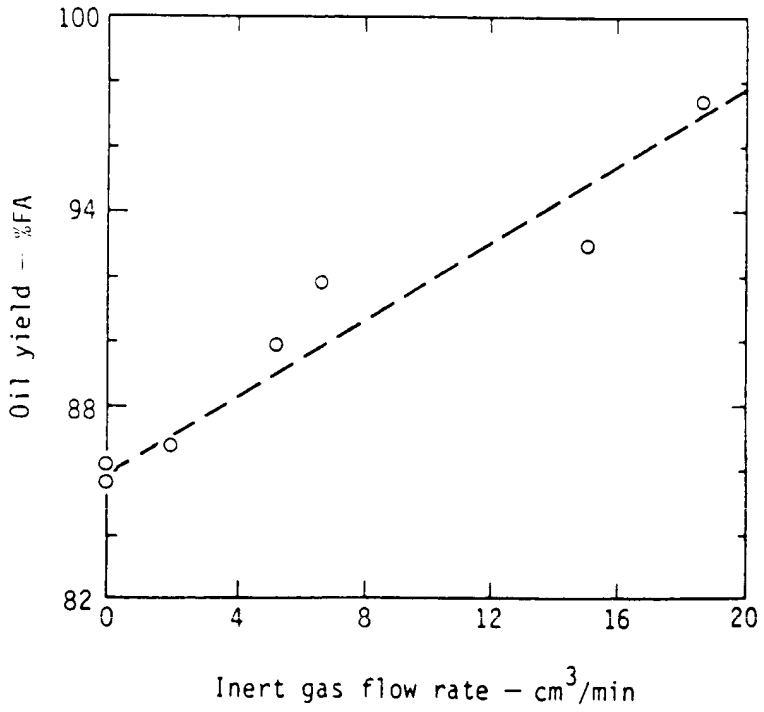

Fig. 7. Oil yield vs external gas flow rate (argon) for powdered oil shale samples heated at 5°C/h. A flow rate of 18 cm^3/min corresponds to about one retort void volume per minute at 400°C and 1 bar.

produces higher self-generated (i.e., autogenous) gas sweep rates during retorting. Furthermore, since the oil products are removed in the vapor phase, the intra-particle flow rate will be approximately proportional to the heating rate. The low permeability of oil shale makes it impossible for an external sweep gas to significantly penetrate a shale block. Autogenous intra-particle gas sweep and oil vaporization processes are the only effective means of removing oil from a block. As a result the more rapid the heating conditions, the faster oil is removed from the block; consequently, less oil degrades.

We were also interested in the effect of the shale grade on yield. To determine this effect, two 17.2-cm diam blocks, one 14 gal/ton and another 47 gal/ton, were retorted at 2°C/hr and compared with experimental data from the approximately 30-gal/ton material (Table 2, Fig. 8). To within experimental error, the yield is independent of grade over the 14- to 49-gal/ton range.

In summary, the experimental data show that oil degradation depends principally on heating rate (as it affects the autogenous gas sweep rate) and not on particle size or grade for the material

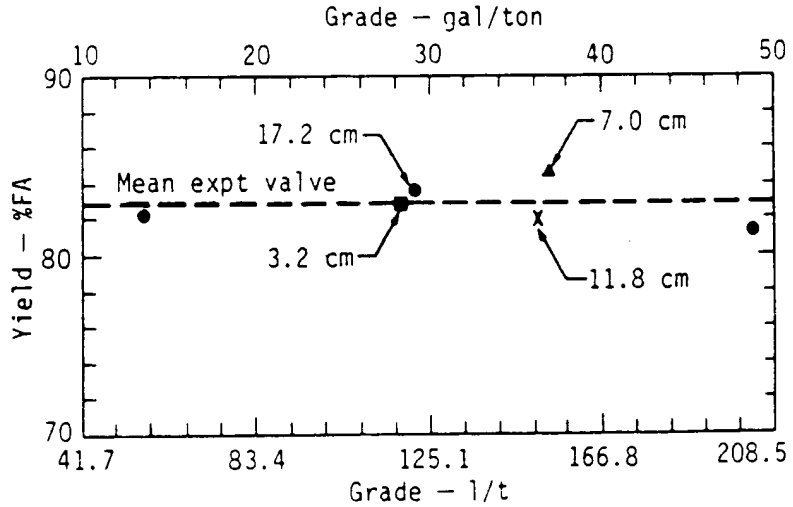

Fig. 8. Oil yield (as percent of Fischer Assay) vs grade (gal/ton, (l/t)), for oil shale particles heated at a rate of 2°C/h.

used here. (Note that particle size may have an important effect on oil degradation because of combustion. Oxidation, however, is an extra-particle effect — here we discuss only intraparticle oil degradation. In a later section, the possible effect of heating rate on oil oxidation is discussed.)

Intraparticle oil degradation — cracking vs coking reactions

A realistic picture of oil release from oil shale can be developed only when one understands the mechanism of intraparticle oil degradation. By determining the mechanisms that lead to major oil loss, one can then attempt to design processing conditions to minimize loss effects.

A recent study[5] of the effects of thermal histories on oil shale pyrolysis showed that the yield was determined by the time-temperature history of the liberated oil and not by the thermal history of the kerogen.[5] Using this work as a basis, we have confined our investigation to the loss in yield due to reactions in the liberated oil.

The principal nonoxidative means by which the liberated shale oil can be degraded are cracking and coking reactions. Because coking and cracking often have slightly different meanings,[16-19] we defined the terms as they will be used here. By cracking we mean vapor phase bond fission reactions that eventually lead to a distribution of molecular units (mostly units smaller than the original molecule) plus, possibly, some carbonaceous residue. Coking we define as liquid or condensed phase reactions resulting in the fusion of two or more molecular species with the ultimate formation of a carbonaceous product plus minor amounts of lower molecular weight gases.

An important difference in the preceding two mechanisms is the distribution of final products. As defined, cracking reactions lead to greater evolution of lower molecular weight hydrocarbon fragments (CH_4, C_2H_6, etc.), whereas coking reactions produce mainly a carbonaceous residue.

Experiments reported in Appendices A and B show that coking is the principal intraparticle oil degradation process. Evidence for this comes from several observations, principally:

- Product distribution from powder and block retorting experiments (Appendix A).
- Shale oil distillation at different heating rates (Appendix B).

Proposed oil production mechanism

From the foregoing experimental data and that in the appendices, it is possible to formulate a simple mechanistic picture of oil production and degradation:

$$\text{(Kerogen-bitumen)} \xrightarrow[\Delta H]{k_d} (\text{oil})_{ip} + \text{carbonaceous residue} + \text{gas} \qquad (1)$$

$(\text{oil})_{ip} \xrightarrow{k_c}$ coke + gas

$(\text{oil})_{ip} \xrightarrow{(k_l + k_g)}$ oil produced.

The term $(\text{oil})_{ip}$ refers to the liberated oil in-place (intraparticle). The in-place oil is subjected to two competing processes: oil degradation leading to coke and gas formation, and oil removal from the particle giving recovered product. In the event of negligible degradation the oil produced would equal 100% of Fischer Assay.

The experimental results in the preceding section show that coke is formed primarly from the oil liquid or condensed phase. Therefore, one can rewrite the oil generation and degradation steps given in Eq. (1) as follows:

$$\text{Oil precursors} \xrightarrow{k_d} \text{oil}^l + \text{oil}^g \qquad (2)$$

$\text{oil}^l \xrightarrow{k_c}$ coke + gas

$\text{oil}^l \xrightarrow{k_l}$ oil produced.

$\text{oil}^g \xrightarrow{k_g}$ oil produced.

Since we are concerned only with reactions involving oil, the term oil precursors refers to that portion of the kerogen plus bitumen that decomposes to oil (i.e., condensible product at 0°C).

The stoichiometries (Table 4) for the reactions given in Eqs. (1) and (2) were determined from experiment. Details leading to this formulation are given in Appendix C.

In the proposed mechanism, the oil precursors decompose at some rate k_d giving a distribution of oil in the gas (oil^g) and liquid (oil^l) phases. This distribution of products is some function of temperature (X(T)) times the total oil present.

TABLE 4.
Stoichiometries for the Reactions given in Eqs. (1) and (2) of the Text.

Oil generation		
$CH_{1.54}N_{0.028}S_{0.005}O_{0.046}$ Raw shale	$\xrightarrow{k_d}$ 0.2 $CH\,N_{0.066}S_{0.018}$	Carbonaceous residue
	+ 0.725 $CH_{1.56}N_{0.020}S_{0.002}$	Oil
	+ 0.018 CO_2, 0.019 H_2, 0.013 CH_4, 0.014 $C_{3.2}H_{7.5}$	Gas
	+ 0.010 H_2O	Water
Oil degradation		
$CH_{1.56}N_{0.020}S_{0.002}$	$\xrightarrow{k_c}$ 0.83 $CH_{0.2}N_{0.024}S_{0.0024}$	Coke
	+ 0.17 CH_4, + 0.36 H_2	Gas
Oil removal		
$CH_{1.56}N_{0.020}S_{0.002}$	$\xrightarrow[k_l]{k_g}$ $CH_{1.56}N_{0.020}S_{0.002}$	

$$oil^g = (X(T))\ oil \tag{3a}$$

$$oil^l = (1 - X(T))\ oil \tag{3b}$$

The term oil^g here refers to the material that is *above* its boiling point, i.e., material that cannot coexist in liquid-vapor equilibrium at 1 bar and the retort temperature, T. The oil vapor in equilibrium with a liquid oil phase is considered separately in the k_1 rate step.

Since the void space in the sample is small, the vapor products are assumed to exit the material at some rapid rate (k_g) giving "produced" oil.

Inside the shale material, the oil in the liquid phase is subject to two competing reactions: rate, k_c, which leads to coke formation, and k_1 which leads to oil produced. The rate of coking, k_c, is for a reaction and hence varies as exp(-E/RT), whereas k_1 is essentially independent of temperature, depending only on the gas flow rate (or heating rate).

The process governed by the rate k_1 can be considered an evaporation step and represented by:

$$oil^l \underset{1}{\rightleftarrows} oil^{vap} \underset{2}{\rightarrow} \text{oil produced}, \tag{4}$$

where step 2 depends on the flow rate. Oil^{vap} is the vapor material in coexistence with some liquid phase, and hence is distinguished from oil^g, the oil totally in the gas phase — i.e., above its boiling point.

From the above proposed mechanism it is apparent that increasing the flow rate (by either rapid heating or, in the case of powders, introducing an inert gas) increases the rate of oil production and reduces the likelihood of competing coking reactions.

To carry out meaningful calculations using the mechanism in Eq. (2), one must know the values of the various rate constants as well as the boiling point distribution for the produced oil

[i.e., X(T)]. Appendices D and E give detailed descriptions of how values were determined for these various quantities. The rate constants are summarized in Table 5.

Although the mechanism is over-simplified, the complexity of the system precludes a more detailed picture with the data now available. Nevertheless, this simple mechanism helps immensely in forming a picture of the processes that may be occurring, as well as in defining retorting conditions that may lead to low yields.

Analysis of block retorting by a simple mathematical model

In this section we analyze the results from the block experiments using a simple mathematical model. The model incorporates the kinetic results from the powder experiments [Eq. (2) and Tables 4 and 5] and thermal data reported in the literature. The model calculates the volume of evolved oil, the degree of intraparticle oil degration, the coke distribution, and the thermal profile through the material. By carrying out such a numerical analysis we can check the ability of our simplified model to describe the experimental results. If there is good agreement, the model can be used to gain further valuable insight on processing conditions and block sizes leading to optimal oil recovery.

TABLE 5.
Summary of Rate Constants[a] for Proposed Mechanism
[Eq. (2) of text].

$k_d(s^{-1}) = 2.8 \times 10^{13} \cdot \exp(-52400/RT)$

$k_c(s^{-1}) = 3.1 \times 10^{7} \cdot \exp(-35000/RT)$

$k_l(s^{-1}) = a \cdot b$

$a \doteq 0.12\ ^{\circ}C^{-1}$

b = heating rate

$k_g >>> k_l, k_c, k_d$

[a] Activation energies are in cal/mole.

Particle size

To make the problem numerically tractable, we assume the block can be treated as a sphere (i.e., one dimensional). It has been shown[20] that particles with equal dimensions in three directions can be analyzed by assuming that the particle is a sphere with a radius given by

$$r_s = \frac{3V_p}{A_p} \quad , \tag{5}$$

where V_p and A_p are the values for the volume and area of the particle, respectively. The 17.2-cm diam blocks have a length-to-diameter ratio of about one and, therefore, can be treated using this assumption.

Governing equations

The equation describing energy conservation for a solid spherical particle with a chemical heat source is given in Part A of Table 6. The three terms on the right refer to energy transport by conduction, convection, and chemical reaction, respectively.

In the analysis given here the convective heat transport term is assumed to be small and hence is neglected. In Appendix F this assumption is shown to be quite valid for the heating rates and grade of material used here.

The organic reactions and rate of heat generation during retorting of an oil shale particle (below the dolomite and calcite decomposition temperatures) can be described by the set of rate equations given in Parts B and C of Table 6. These equations come directly from the experimentally derived mechanism for oil generation and degradation given in the previous section [Eq. (2)] and the stoichiometries in Table 4.

The density of the shale block at a particular temperature is given by the expression

TABLE 6.
Governing Equations for 1-D Model of Block Retorting.

A. Heat Transport

$$\rho_s C_s \frac{\partial T}{\partial t} = \nabla \cdot k \nabla T - \overline{v_g \rho_g C_g} \nabla T + \dot{q}$$

B. Chemical Reactions

Reaction	Rate Eq.	Physical description
Oil precursors $\xrightarrow{k_d}$ $(1 - X(T)) \cdot Oil^l$	$R_{ol} = f_o(1 - X(T))\, k_d \cdot \rho_{kb}$	Intraparticle oil formation from the organic material (i.e., Kerogen + bitumen) in the shale.
Oil precursors $\xrightarrow{k_d}$ $X(T) \cdot Oil^g$	$R_{og} = f_o \cdot X(T) \cdot k_d \cdot \rho_{kb}$	
$Oil^l \xrightarrow{k_c} (f_c)$ coke	$R_c = f_c \cdot k_c \cdot \rho_{lo}$	Intraparticle oil degradation leading to formation of coke and non-condensable gas.
$Oil^l \xrightarrow{k_c} (1 - f_c)$ gas	$R_g = \frac{(1 - f_c)}{f_c} R_c$	
$Oil^l \xrightarrow{k_l}$ Oil produced $Oil^g \xrightarrow{k_g}$ Oil produced	$R_{op} = R_{og} + k_l \cdot \rho_{lo}$	Oil evolution from the block.

C. Rate of Heat Generation

$$\dot{q} = \nabla H \cdot k_d \cdot \rho_{kb}$$

$$\rho_s(T) = \rho_{min} + \rho_{org} \quad . \tag{6}$$

Assuming negligible decomposition of mineral species ($T < 600°C$), the block density can be written as:

$$\rho_s(T) = \rho_s^o - \rho_{vol}(T) \tag{7}$$

where ρ_s^o is the initial block density. The volatile mass loss under zero degradation conditions (i.e., 100% FA, by definition) is given by ρ_{vol} where

$$\rho_{vol}(T) = 0.78\ (1 - F)\ \rho_{kb}^o \quad . \tag{8}$$

The coefficient 0.78 represents the mass fraction of volatile matter released per unit weight of initial organic material.[21] At the end of retorting the intraparticle oil has either vaporized or coked and hence:

$$\rho_s^f = \rho_s^o - \rho_{vol} \quad . \tag{9}$$

This system of equations describing the particle retorting process was solved using a partial differential equation routine implemented by Sincovec and Madsen.[22] The particle was zoned into 21 equal-volume segments. The assumed boundary conditions are

$$\frac{\partial T}{\partial r}\Big)_{r=0} = 0 \tag{10}$$

and

$$T\Big)_{r=r_s} = T_0 + bt. \tag{11}$$

The second boundary condition, Eq. (11), is set by the experiment, where T_0 is the initial block temperature and b is the heating

rate determined from the thermocouple readings near the block edge ($r/r_s \doteq 0.97$).

The other necessary initial conditions include the block density and concentration of organic matter. The block density was determined experimentally (see experimental section), and the concentration of organic matter was calculated from the oil grade using the correlation reported by Stanfield *et al.*[23]

Oil shale physical properties

The heat capacity of the shale is taken to be:

$$C_s = [(216.8 + 120.9\ W_k)\cdot(1.0 - F) + 197.8\ F] + [(0.1478 + 1.329\ W_k)\cdot(1.0 - F) + (0.220\ F)]\cdot[T - 298] \quad , \tag{12}$$

where W_k is the weight fraction of kerogen in the raw shale and F is the fractional conversion (decomposition) of kerogen at temperature T. This equation is also from the analysis by Carley[24] of the Wise *et al.*[25] data.

The thermal conductivity of the shale is assumed to be given by

$$k = 1.25 \times 10^{-4}\cdot(1 - F) + 0.83 \times 10^{-4}\ F \quad , \tag{13}$$

based on data reported by Tihen *et al.*[26] for 30-gal/ton material.

Model calculation vs experimental results

It is important to note that there are no free parameters in the model. All input to the model was from experimental results given here (e.g., kinetics from powder shale experiments) or data previously reported in the literature (e.g., heat capacity,

thermal conductivity, etc.). Therefore, a comparison of the calculated and experimental results provides a sensitive test of the model.

Oil evolution and temperature distribution

Plotted in Figs. 9 and 10 are calculated and experimental results showing the oil evolution, total oil yield, and temperature data for a set of block retorting experiments. The

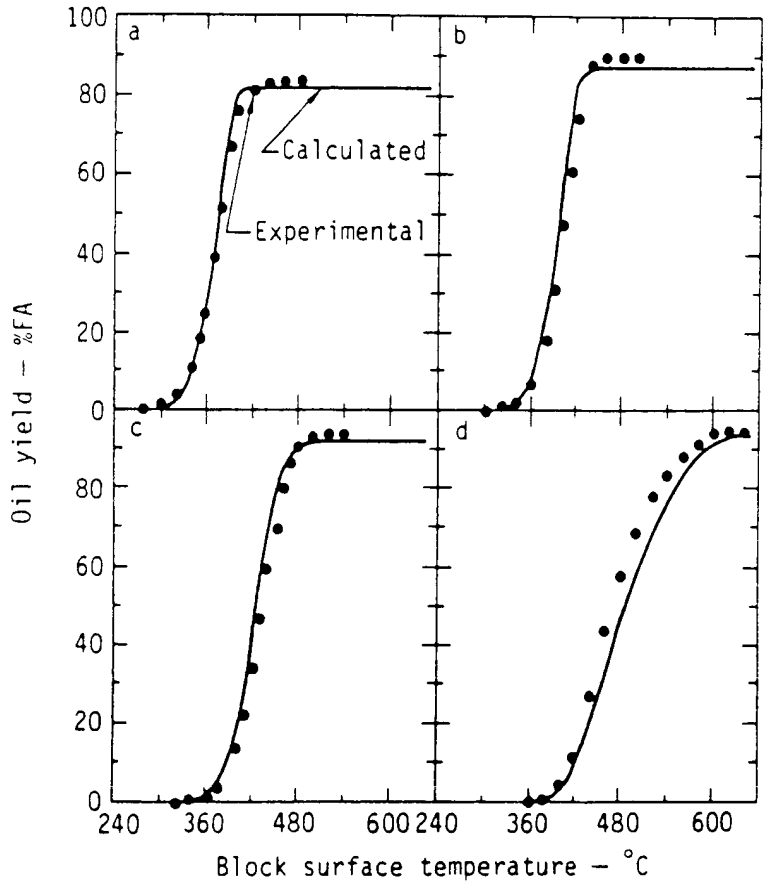

Fig. 9. Oil evolution vs block surface temperature calculated using mathematical model and observed experimentally for surface heating rates of (a) 2, (b) 6, (c) 18, and (d) 60°C/h. Blocks are 17.2-cm diam and 29 to 33 gal/ton. The experimental points are from Figure 5.

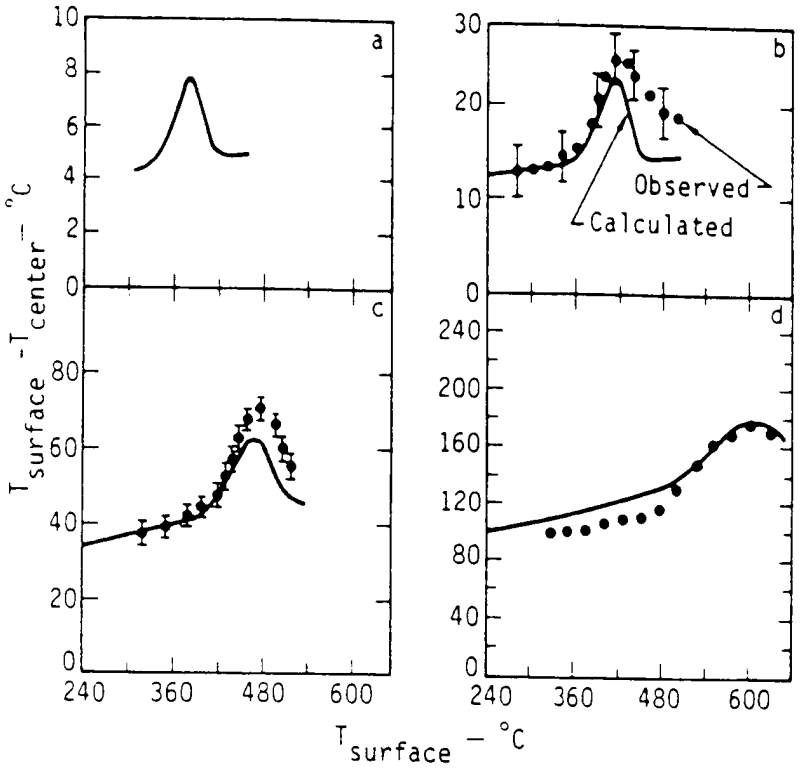

Fig. 10. Temperature difference between block surface and center vs block surface temperature, calculated using mathematical model and observed experimentally (•) for heating rates of (a) 2, (b) 6, (c) 18, and (d) 60°C/h. Blocks are 17.2-cm diam. The blocks are the same as those referred to in Fig. 9.

experimental data are for the 17.2-cm diam blocks heated at rates of 2, 6, 18, and 60°C/min [corresponding to sample Nos. III-38, 18, 30, and 63, respectively (Table 2)]. The grade of the blocks ranged from about 29 to 33 gal/ton.

The calculated evolution of oil vs block surface temperature agrees well with the experimental results (Fig. 9). The biggest discrepancy between the model calculation and experimental data is for the high heating rate experiment (1°C/min). The model predicts oil release at a slightly higher temperature (~20°C) than is observed experimentally. In all other cases, however, the experimental and calculated evolution profiles agree to

within 10°C. Furthermore, the calculated effect of heating rate on total oil yield agrees with the experimental results.

The measured and calculated temperature difference between the block surface and center is shown in Fig. 10. The data are plotted vs the block solid surface temperature. The conditions correspond to those in Fig. 9. Temperature difference was chosen to represent the thermal data, since it provides a more sensitive comparison between calculated and experimental results than do temperature profiles.

The agreement between the calculated and observed temperature values is quite good. In all cases the model predicts the block center temperature to within just a few degrees.

The biggest discrepancies appear near the end of oil evolution; this may indicate the occurrence of other endothermic reactions (e.g., pyrolytic gas evolution from the carbonaceous residue or carbonate decomposition) and/or an incorrect value for the thermal conductivity of the spent shale.

Accurate data for the difference between block center and surface temperatures were not available for the heating rate of 2°C/hr. The error in the thermocouple readings was too large to quantitatively determine a difference except to note that it was less than 10 to 15°C, hence only calculational results are shown in Fig. 10(a).

Carbon distribution in spent shale

The radial distribution of organic carbon in the spent shale blocks was determined at the completion of several retorting experiments. Analyses were performed on drill corings taken at different radial positions; the procedure used in the coring operations is similar to that reported by Mallon and Braun.[27]

Shown in Fig. 11(a) and (b) are typical results for two 17.2-cm diam cylindrical blocks heated at rates of 2 and 60°C/hr. The circles represent experimental data, whereas the lines are results from model calculations. The interesting

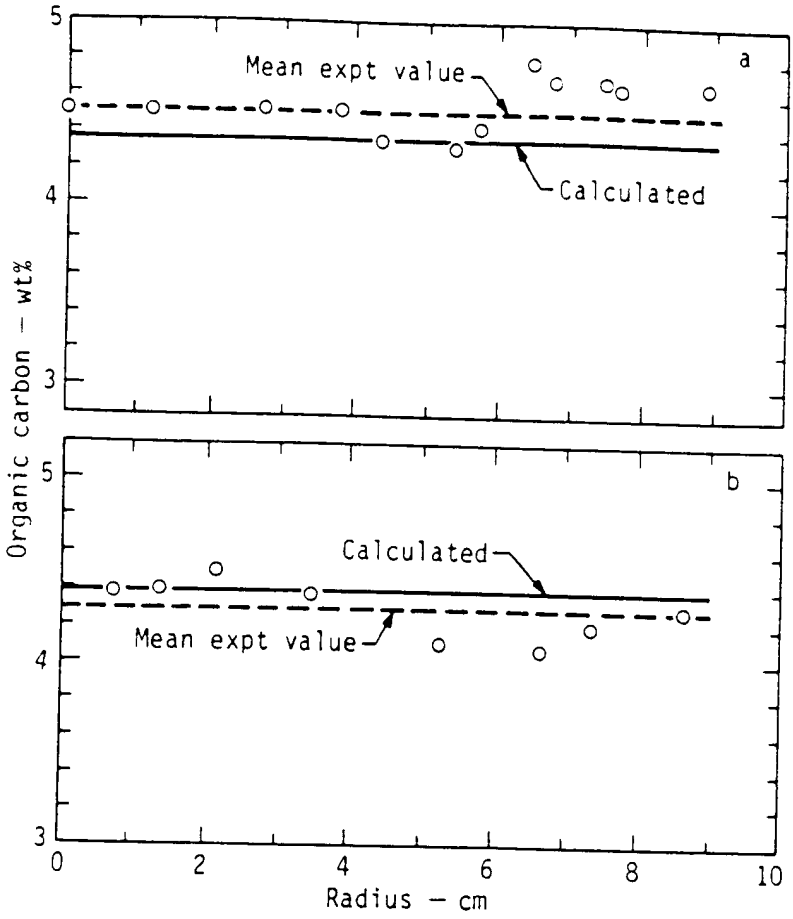

Fig. 11. Weight percent organic carbon remaining in spent shale vs radial position in a 17.2 cm diameter shale particle. The straight line is from a model calculation and open circles represent experimental data for 121.8 and 156.4 l/t (29.2 and 37.5 gal/ton) blocks heated at (a) 2 and (b) 60°C/h, respectively.

feature is that the concentration of organic carbon residue is independent of radial position in the block. This phenomena was also observed in blocks having a smaller diameter. See, for example, Fig. 12 for a 7.2-cm diam block. (It was not possible to use the 1-D model for the 7.2-cm block since the length-diameter ratio was 2.5. Therefore, the solid line in Fig. 12 was determined from the observed yield loss and the calculated organic carbon converted to char — see Table A2 of Appendix A).

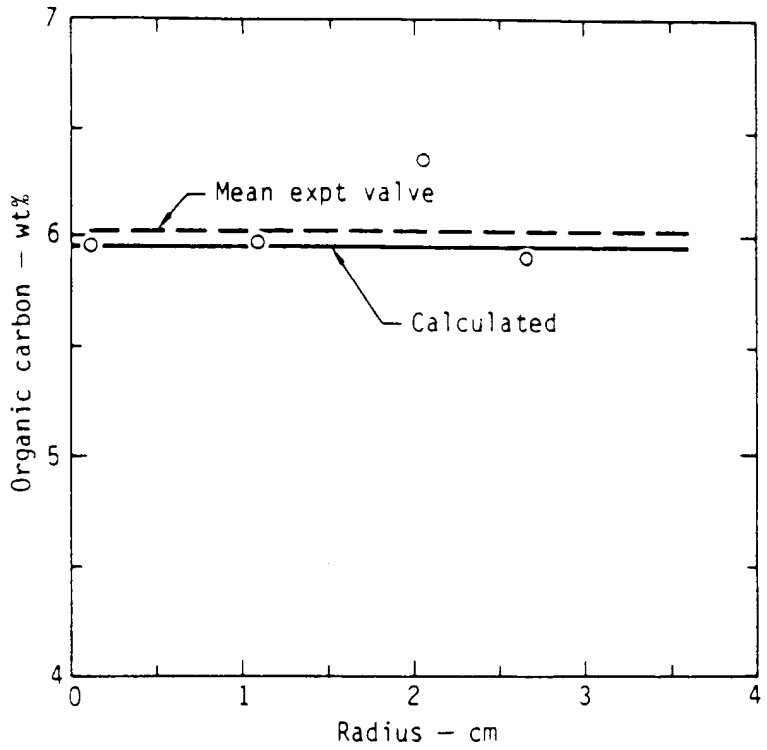

Fig. 12. Weight percent organic carbon remaining in spent shale vs radial position in a 156.0 l/t (37.4 gal/ton), 7.2 cm diameter cylindrical block. The solid line was calculated and the circles represent experimentally observed values. The heating rate was 2°C/h.

The spatial independence of organic carbon deposition indicates that the oil that degrades is apparently not diffusing through the block, but instead remains near the site of initial formation. This observation supports the proposed mechanism for oil degradation [eq. (2)]. The mechanism assumes that the oil degradation due to coking occurs in the relatively immobile condensed or liquid phase and not in the mobile gas phase; hence, the mechanism predicts a spatially independent deposition of carbon during retorting (for a near constant heating rate throughout the particle).

From the preceding data it becomes clearer why particle size has little effect on oil yield. Since the degradation process

is not occurring in the gas phase, longer intraparticle residence times (i.e., larger blocks) have little effect on the degradation process. This conclusion pertains only to block sizes and heating rates similar to those used in this study. One can easily think of conditions (e.g., very fast heating rates and/or large blocks) where the surface temperature of the shale becomes very hot (>700°C) while the inside is still retorting. Under these conditions, cracking of the gas phase products diffusing from the interior of the block may be an important oil degradation process. It is also probable that extraparticle oil combustion will become a major oil loss mechanism.

Water evolution during block retorting

The amount of water released during retorting of the 17.2-diam blocks is given in Table 7. The weight of water released is about 1.9% of the total weight loss (to ~500°C) from the 29- to 37-gal/ton material.

The dynamics of water evolution above 240°C were recorded during two of the slow retorting experiments. The water is released in approximately equal amounts in two steps (Fig. 13)

TABLE 7.
Quantity of Water Released during Retorting of 17.2-cm diam Blocks

Run No.	Grade, gal/ton	H_2O yield ml H_2O/kg raw shale
III-2	29.0	25
III-18	32.4	21
III-30	33.3	17
III-38	29.2	17
III-63	37.5	17
III-55	13.8	12
III-81	48.8	14[a]

[a] Accurate determination of the total water released was complicated by the large quantity of oil evolved. Hence, this number represents a lower limit on the total water evolved.

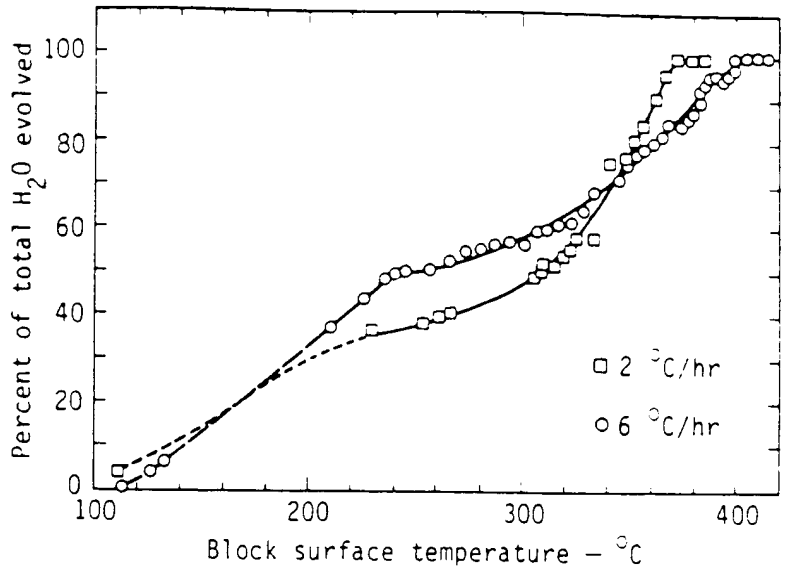

Fig. 13. Volume of water released (as % of total) vs block surface temperature for a 133.5 and 121.0 l/t (32 and 29 gal/ton) shale blocks (17.2 cm diameter) heated at 2 and 6°C/h, respectively.

one below ~240°C and the second during retorting (i.e., above 240°C).

Note the similarities in the evolution profiles for the water with those for oil (Fig. 5). The water released at high temperatures (>240°C) apparently forms during the kerogen decomposition process. The water released below 240°C may come from hydrated mineral species or nahcolite in the shale.

Practical implications of the results

The results of this study have a great deal of practical significance for proposed methods of *in-situ* shale processing. As mentioned in the introduction, there are two principal means of processing shale: combustion and hot inert gas retorting. The movement of the pyrolysis front during combustion retorting is quite fast, the shale heating rates being of the order of several degrees per minute. On the other hand, heating rates

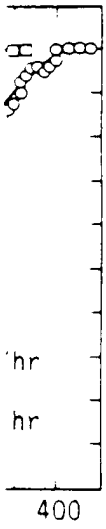

during hot inert gas retorting may be much slower — only a few degrees (or few tenths of a degree) per hour.

From the results of this study it is apparent that significant intraparticle degradation may occur during hot gas retorting, whereas relatively little will probably result from combustion processing.

A least-squares fit of the data for oil yield vs logarithm of the heating rate (data are from both powders and blocks — Fig. 6 and Tables 2 and 3) gives a valuable empirical relation that can be used to estimate the intraparticle yield loss at various heating rates:

$$\begin{aligned} YL &\doteq 100 - [81.1 + 8.24\ (\log b)], \\ &\qquad b \leq 190°C/hr \\ YL &\doteq 0.0,\ b > 190°C/hr. \end{aligned} \tag{14}$$

Furthermore, the percent organic carbon converted to char within the block can be estimated as

$$\begin{aligned} OC_{char} &= -0.606 \cdot (81.1 + 8.24 \log b) \\ &\qquad + 80.54, \\ &\qquad b \leq 190°C/hr \\ &= 19.9, \qquad b > 190°C/hr. \end{aligned} \tag{15}$$

The above expressions are valid over the range of heating rates, particle size, and grade of material used in this study. Caution should be used in applying these relationships to very large shale particles, since the material used in this study was less than 18-cm diam. LLL is currently conducting experiments to check the validity of this work when applied to particles approaching 60-cm (2 ft) diam.

The data here also only apply to intraparticle degradation. Oxidation of the oil once it leaves the blocks (extraparticle) can become important for large size material processed at a high

heating rate. Under this condition, a large thermal gradient develops, resulting in kerogen pyrolysis occurring on the interior of the block while the exterior is being oxidized (i.e., burned). LLL is currently developing a detailed retorting model that takes into account both of these processes.

SUMMARY AND CONCLUSIONS

The principal conclusion of this study is that particle size (up to 17.2 cm) and grade (14 to 49 gal/ton) have little effect on the degree of intraparticle oil degradation during shale retorting. On the other hand, the rate at which the shale is heated has a pronounced effect on yield. For example, retorting at a rate of 180°C/hr gives a yield of ~99%, while retorting at 2°C/hr gives only about 83% yield.

The principal degradation product is a carbonaceous residue, which we term coke. Evidence shows that oil degradation occurs mainly in the liquid or condensed phase (coking) and not in the vapor phase (cracking). Furthermore, the degree of degradation is controlled by the rate of autogenous (i.e., self-generated) *internal* gas sweep through the particle, which in turn is controlled by the rate of particle heating. Therefore, higher heating rates generate greater intraparticle gas sweep rates and less oil degradation.

A mechanism is proposed to explain the observed degradation of oil during retorting. Rate equations characterizing the various mechanism steps are determined from experimental data on powdered shale and incorporated into a mathematical model describing oil shale block retorting. The model contains no free parameters. Calculations carried out with the use of the model agree very well with experimental results.

ACKNOWLEDGMENTS

The authors acknowledge the fine technical support of S. Santor, J. Taylor, and P. Rossler in carrying out certain

phases of this work. The excellent analytical work by L. Gregory is also deeply appreciated.

This work was supported by the U.S. Department of Energy (DOE) under contract No. W-7405-Eng-48.

FOOTNOTES

*Reference to a company or product name does not imply approval or recommendation of the product by the University of California or the U.S. Department of Energy (DOE) to the exclusion of others that may be suitable.

SYMBOL LIST

A_p = particle surface area (m^2)
C_s = shale heat capacity (kcal/kg K)
C_g = heat capacity of evolved gaseous products (kcal/kg K)
E = activation energy (kcal/mole)
F = dimensionless fraction of decomposed kerogen
ΔH = enthalpy of kerogen decomposition (kcal/kgm)
OC_{char} = percent organic carbon converted to char
R_{ol} = rate of liquid oil formation (intraparticle) ($kg/s \cdot m^3$)
R_{og} = rate of gas phase oil formation (intraparticle) ($kg/s \cdot m^3$)
R_c = rate of intraparticle coke formation ($kg/s \cdot m^3$)
R_g = rate of non-condensible gas formation during coking ($kg/s \cdot m^3$)
R_{op} = rate of oil release from the particle ($kg/s \cdot m^3$)
T = temperature (K)
T_o = initial particle temperature (K)
V_p = particle volume (m^3)
W_k = weight fraction kerogen in raw shale
X = fraction of liberated oil totally in the gas phase
1-X = fraction of liberated oil as liquid or in liquid-vap equilibrium.
YL = precent oil yield loss

b = heating rate (K/s)

f_o = fractional conversion of kerogen-bitumen to oil

f_c = fractional conversion of degraded oil to coke

k = shale thermoconductivity (kcal/s·m·K)

k_d = rate constant for oil generation (s^{-1})

k_l = rate constant for oil production via liquid vaporization (s^{-1})

k_g = rate constant for oil production as initial gas products (s^{-1})

k_c = rate constant for coke formation (s^{-1})

$\dot{q}$ = rate of heat generation (kcal/s·m^3)

r = radial position (m)

r_o = block radius (m)

r_s = radius of equivalent spherical particle (m)

t = time (s)

ρ_s = density of shale particle (kg/m^3)

ρ_{min} = mass concentration of mineral matter (kg/m^3)

ρ_{org} = mass concentration of organic matter (kg/m^3)

ρ_s^o = initial shale particle density (kg/m^3)

ρ_s^f = final shale particle density (kg/m^3)

ρ_{lo} = mass concentration of intraparticle liquid oil (kg/m^3)

ρ_{kb}^o = initial mass concentration of kerogen + bitumen (kg/m^3)

ρ_{vol} = mass concentraion of kerogen + bitumen converted to volatile products (kg/m^3)

$\overline{\rho_g v_g}$ = average mass flux rate of gas products from shale (kg/m^2sec)

REFERENCES

1) Lewis, A. E. and A. J. Rothman, "Rubble In-Situ Extraction (RISE): A Proposed Program for Recovery of Oil from Oil Shale," Lawrence Livermore Laboratory, Rept. UCRL-51768 (1975).

2) Rothman, A. J., "Research and Development on Rubble In-Situ Extraction of Oil Shale (RISE) at Lawrence Livermore Laboratory," Colorado School of Mines Quarterly 70, 159 (1975).

3) Rothman, A. J., Ed., "Quarterly Report LLL Oil Shale Program, October – December 1975," Lawrence Livermore Laboratory, Rept, UCID-16986-75-2 (1976).

4) Nuttall, H. E., "Mathematical Model and Experimental Investigation of In-Situ Shale Retorting," in Proc. Annual Fall Technical Conf. and Exhibition of the Soc. Pet. Eng. AIME, 51st, New Orleans, Louisiana, 1976, Paper No. SPE 6064.

5) Stout, N. D., G. H. Koskinas, J. H. Raley, S. D. Santor, R. J. Opila, and A. J. Rothman, "Pyrolysis of Oil Shale: The Effects of Thermal History on Oil Yield," Colorado School and Mines Quarterly, 71, 153 (1976).

6) Hill, G. R., D. J. Johnson, M. Lowell, and J. L. Douglas, "Direct Production of a Low Pour Point High Gravity Shale Oil," Ind. Eng. Chem. Product Res. and Dev., 6, 52 (1967).

7) Cummins, J. J., and W. E. Robinson, "Thermal Degradation of Green River Kerogen at 150 to 350 °C; Rate of Product Formation," U.S. Bureau of Mines, Rept. Investigation 7620 (1972).

8) Johnson, W. F., D. K. Walton, H. H. Keller, and E. J. Couch, "In-Situ Retorting of Oil Shale Rubble: A Model of Heat Transfer and Product Formation in Oil Shale Particles," Colorado School of Mines Quarterly, 70, 237 (1975).

9) Needham, R. B., A. Judzis, and A. J. Cornelius, "Oil Yield and Quality from Simulated In-Situ Retorting of Green River Oil Shale," Proc. Annual Fall Tech. Conf. and Exhibition of the Soc. Pet. Eng. AIME, 51st, New Orleans, Louisiana, 1976, Paper No. SPE 6069.

10) Huang, E. T. S., "Retorting of Single Oil Shale Blocks in Nitrogen and Air," IECEC Inter-Society Energy Conversion Conf., 11th, Stateline, Nevada, 1976 (to be published).

11) Mallon, R. G., and W. C. Miller, "Thermal Behavior of Oil Shale Heated in Air," Colorado School of Mines Quarterly, 70, 221 (1975).

12) Minster, R. A., R. A. Martel, and A. E. Harak, "Some Observations of Retorting Phenomena in Shale Blocks," Laramie Energy Research Center, Laramie, Wyo, Rept. LERC/R1-76/8 (1976).

13) Smith, J. S., "Theoretical Relationship Between Density and Oil Yield for Oil Shales," U.S. Bureau of Mines, Rept. of Investigation 7248 (1969).

14) Stout, N. D., G. H. Koskinas, and S. D. Santor,"A Laboratory Apparatus for Controlled Time/Temperature Retorting of Oil Shale," Lawrence Livermore Laboratory, Rept. UCRL-52158 (1976).

15) Campbell, J. H., and T. T. Coburn, "Oil Shale Retorting III. Variation in Shale Oil Chemical and Physical Properties During Retorting of Blocks," Lawrence Livermore Laboratory, Rept. UCRL-52256-2, (1976).

16) Nelson, W. L., Petroleum Refinery Engineering, McGraw-Hill Book Co., New York, 1958, 4th ed.

17) Kobe, K. A., and J. J. McKetta, Jr., Advances in Petroleum Chemistry and Refining, Interscience, New York, 1962, vol. VI.

18) Lowry, H. H., Ed., Chemistry of Coal Utilization, Supplementary Volume, John Wiley & Sons, Inc., New York, 1963, Ch. 4 and 9 and references cited therein.

19) Martin, S. W., and L. E. Wills, "Coking Petroleum Residues," in Advances in Petroleum Chemistry and Refining, K. A. Kobe and J. J. Miketta, Jr., Eds., (Interscience, New York), vol 2, (1959).

20) Sohn, H. Y., and J. Szekely, Chem. Eng. Sci. 27, 763 (1972).

21) Allred, V. D., "Compositional Diagrams: A Method for Interpretation of Fischer Assay Data," Amer. Chem. Soc. Meeting, Div. of Fuel Chemistry Preprints 21, 55 (1976).

22) Sincovec, R. F., and N. K. Madsen, ACM Transactions on Mathematical Software 1, 232 (1975).

23) Stanfield, K. E., I. C. Frost, W. S. McAuley, and H. N. Smith, "Properties of Colorado Oil Shale," Bureau of Mines Rept. of Investigation 4825 (1951).

24) Carley, J., private communication, Lawrence Livermore Laboratory (1976).

25) Wise, R. L., R. C. Miller, and H. W. Sohns, U.S. Bureau of Mines Rept. of Investigation 7482 (1971).

26) Tihen, S. S., H. C. Carpenter, and A. W. Sohns, Proc. 7th Conf. Thermal Conductivity, National Bureau of Standards Special Publ. No. 302, (1968) p. 529.

27) Mallon, R. G., and R. L. Braun, "Reactivity of Oil Shale Carbonaceous Residue with Oxygen and Carbon Dioxide," Colorado School of Mines Quarterly, 71, 309, (1976).

28) Smith, J. W., U.S. Bureau of Mines, Rept. of Investigation 5725 (1961).

29) Campbell, J. H., G. Koskinas, N. Stout, "The Kinetics of the Decomposition of Colorado Oil Shale 1. Oil Generation," Lawrence Livermore Laboratory, Rept. UCRL-52089 (1976).

30) Raley, J., and R. Braun, "Oil Degradation During Oil Shale Retorting," Lawerence Livermore Laboratory, Rept. UCRL-78098 (1976).

31) Hindmarsh, A. C., "Gear: Ordinary Differential Equation System Solver," Lawrence Livermore Laboratory, Rept. UCID-30011, Rev. 3 (1974).

APPENDIX A. EVIDENCE FOR COKING: ORGANIC CARBON DISTRIBUTION IN RETORTING PRODUCTS

The amount of organic carbon converted to char under various retorting conditions is given in Table A1 for powders and Table A2 for four of the block experiments. Stout *et al.*[5] reported that 83% of the carbon lost from oil by degradation processes appears as char and 17% as gas (mainly CH_4). Furthermore, they showed that the percent organic carbon converted to char (OC_{char}) could be correlated with oil yield by the empirical relation:

$$OC_{char} = -0.606 \cdot OY + 80.514,$$

where OY is the oil yield as percent FA. Using this correlation, a predicted value of organic carbon converted to char has been calculated for the experiments in Table A1 and A2. As shown in the tables, the agreement between the predicted and observed values is quite good.

TABLE A1.
Summary of Oil Shale Powder Experiments (22 gal/ton material[a]); Linear Heating Conditions (i.e., dT/dt = const).

Sample No.	Heating rate, °C/hr	External flow[c] rate, cm^3/min	Oil yield, % FA	Predicted[b] % organic carbon converted to char, %	Oil wt % C	Oil wt % H	Oil wt % N	Oil wt % S	Char wt % Total C	Char wt % H	Char wt % Acid CO_2	Char wt % Organic C	Observed % organic carbon converted to char, %
RP-1	0.60	0	78.8	32.8	85.85	12.74	1.56	—	10.22	0.21	24.40	3.56	32.4
TC-22	5.0	0	86.1	28.3	84.38	12.00	1.59	0.39	9.67	0.28	24.35	3.03	27.6
TC-18	5.0	0	85.7	28.6	84.85	12.45	1.60	0.62	9.66	0.28	24.35	3.02	27.4
TC-20	19.3	0	90.8	25.5	83.54	11.98	1.64	0.45	9.46	0.22	24.42	2.80	25.3
TC-14	63.5	0	96.1	22.3	85.86	12.08	1.75	0.54	9.32	0.20	24.57	2.62	23.6
TC-12	185.0	0	98.4	20.9	86.51	11.66	1.56	0.40	9.01	0.17	24.58	2.31	20.8
Fischer Assay	720	0	100.0	19.9	86.38	11.22	2.06	—	8.84	0.19	24.30	2.21	19.9
TC-28	5	2.0	86.7	28.0	86.17	11.98	1.71	0.40	9.70	0.18	24.35	3.06	27.7
TC-52	5	5.2	89.8	26.1	84.07	12.12	—	0.62	9.59	0.18	24.62	2.87	26.0
TC-34	5	7.0	91.9	24.8	84.65	11.62	1.79	0.31	9.62	0.18	24.52	2.93	26.6
TC-38	5	18.6	97.4	21.5	83.60	11.65	1.85	0.57	9.50	0.15	24.44	2.84	25.8
TC-56	5	15.0	92.9	24.2	84.88	12.36	1.74	—	—	—	—	—	—
TC-48	19.3	0	91.0	25.6	84.87	11.94	1.83	0.58	9.57	0.20	24.68	2.84	25.7

[a] 9.914 wt% organic carbon in raw shale.

[b] Based on paper by Stout *et al.*[5], % organic carbon (converted to coke) = -0.606 × oil yield + 80.54.

[c] A zero flow indicates autogenous conditions.

TABLE A2.
Organic Carbon Converted to Char for Several Block Retorting Experiments.

Sample[a]	Grade, gal/ton	Heating rate °C/hr	Yield, % FA	% organic carbon converted to char	
				Measured	Predicted[b]
III-2	29.0	180	99.0	20.3	20.5
III-38	29.2	2	83.8	29.3	29.7
III-63	37.5	60	96.0	20.2	22.3
III-85	37.4	2	84.9	29.4	29.1

[a]Block dimensions are given in Table 2 of main text.

[b]Based on work by Stout *et al.*[5], organic carbon converted to char = (-0.606 × oil yield) + 80.54.

The important point is that over 80% of the carbon lost from the oil goes to form carbonaceous residue — this strongly indicates coking as the major oil degradation process. Furthermore, Stout *et al.*[5] found that the H_2 concentration in the evolved gas increased by roughly twofold with a 20% loss in FA yield. There was no observable increase in C_n, $n > 1$, gas phase hydrocarbons. Hence, it is probable that for the experiments reported here, little loss in yield results from cracking of the produced oil.

APPENDIX B. EVIDENCE FOR COKING: SHALE OIL DISTILLATION EXPERIMENTS

Coking of shale oil is readily observed when distilling it at various heating rates. Shown in Fig. B1 is the weight precent coke produced vs log of the heating rate during distillation of shale oil at 1 bar. Also plotted (---) is the equivalent amount of carbonaceous residue formed by oil degradation during retorting of shale powders. The dashed curve was obtained using the expressions:

$$\text{weight \% coke} \doteq YL \cdot (0.83) \cdot (13.0/13.5) \quad ,$$

[b]Based on paper by Stout *et al.*[5], % organic carbon (converted to coke) = -0.606 × oil yield + 80.54.

[c]A zero flow indicates autogenous conditions.

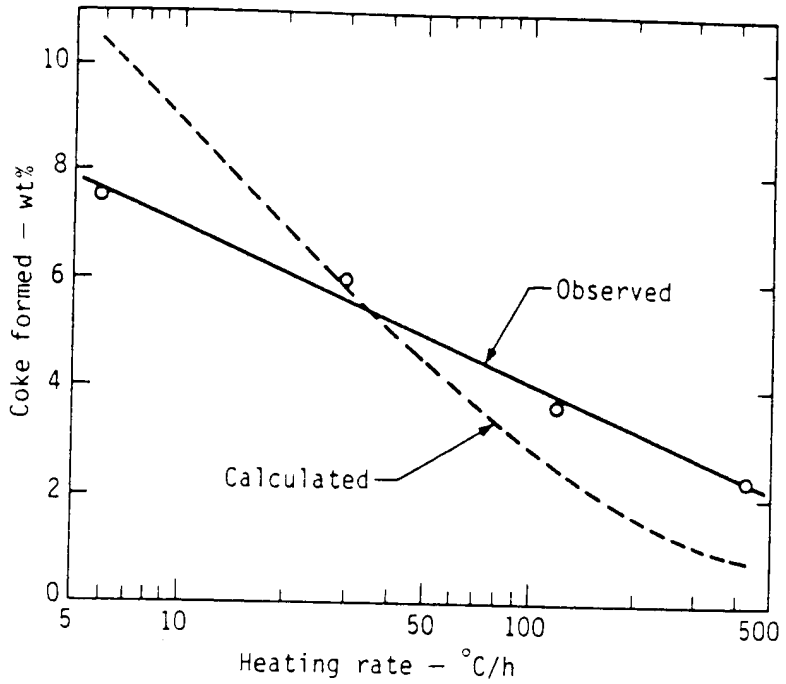

Fig. B1. (-o-) weight percent coke produced during distillation of shale oil at different heating rates and (---) calculated wt% coke formed by retorting powdered shale.

where YL is the percent yield loss observed at a given heating rate (Fig. 6), 0.83 is the fractional conversion of organic carbon in oil to organic carbon in coke, and 13.0 and 13.5 are approximate empirical weights for 500°C carbonaceous residue (CH) and oil ($CH_{1.5}$), respectively.

The agreement between the weight of carbon residue formed by retorting powdered shale and coking shale oil is quite good. This tends to further support coking as the major intra-particle oil degradation process.

APPENDIX C. REACTION STOICHIOMETRIES

We have recently reported the organic carbon distribution and elemental composition for the oil, char, and gas produced during pyrolysis of oil shale.[5] For a typical Fischer Assay

heating schedule (12°C/min), 20% of the organic carbon orginally present in the kerogen is converted to char, 72.5% to oil, and 7.5% to gas. The oil and char elemental compositions are $CH_{1.56}N_{0.020}S_{0.003}$ and $CHN_{0.066}S_{0.022}$, respectively and the gas is 24.2% CO_2, 26.1% H_2, 18.4% CH_4, and 25.9% $\sum_{n>2} C_n$ by volume (average composition for $\sum_{n>2} C_n = C_{3.2}H_{7.5}$). On the basis of these results and the elemental composition of kerogen,[28] one can write the following stoichiometric equation for the decomposition of kerogen (Fischer Assay yield):

$$CH_{1.54}N_{0.028}S_{.005}O_{.046} \xrightarrow{k_d} \begin{cases} 0.725\ CH_{1.56}N_{.020}S_{.002} & \text{Oil} \\ +\ 0.2\ CHN_{.066}S_{.018} & \text{Residue} \\ +\ 0.018\ CO_2 \\ +\ 0.019\ H_2 \\ +\ 0.013\ CH_4 \\ +\ 0.014\ C_{3.2}H_{7.5} \end{cases} \text{Gas}$$
$$+\ 0.010\ H_2O \qquad \text{Water.}$$

Only very slight adjustments needed to be made in the observed elemental and gas compositions for the equation to balance. The water product was added to close the hydrogen balance.

We also found[5] that during oil degradation 83% of the carbon lost from oil appeared as coke and 17% as gas in the form of CH_4. Evolution of considerable quantities of hydrogen was also observed.

The coke formed during oil degradation is lower in hydrogen content than the carbonaceous residue from a Fischer Assay. The carbonaceous residue has an H/C ratio of about one, whereas the coke plus carbonaceous residue from a 79% oil yield experiment has an H/C ratio of only 0.70. From the results in Table A1 of Appendix A

one can calculate a coke H/C ratio of about 0.2. Hence, the oil degradation reaction can be written as:

$$CH_{1.56}N_{0.020}S_{0.002} \xrightarrow{k_c} 0.83\ CH_{0.2}N_{0.020}S_{0.002} + 0.17\ CH_4 + 0.36\ H_2$$

APPENDIX D. RATE CONSTANTS FOR OIL GENERATION AND DEGRADATION CALCULATIONS

The rate constants for the proposed mechanism were determined using data from powder experiments. All reactions were treated as first order.

The rate of oil generation has recently been reported by Campbell *et al.*[29] and found to have a rate constant:

$$k_d\ (s^{-1}) = 2.81 \times 10^{13} \exp(-52400/RT). \qquad (1D)$$

As a first approximation the rate constant for coking, k_c, was assumed to be equal to that reported by Raley and Braun for asphalts.[30] The temperature dependence (i.e., activation energy) of this rate data, however, is too high and predicts <10% difference in yield over a change in heating rate of 720 to 1°C/hr. The observed yield loss is ~20% (Fig. D1). By using a lower temperature dependence for the coking rate (E = 35 kcal/mole) one can predict the observed yield losses with decrease in heating rate. The value of the rate constant at 350°C, however, is still assumed to be given by that for asphalt coking (i.e., 1.6×10^{-5} sec^{-1}); k_c is then:

$$k_c\ (s^{-1}) = 3.1 \times 10^7 \cdot \exp\left(\frac{-35000}{RT}\right). \qquad (2D)$$

Since k_g is much greater than the other rate constants, it has no influence on the calculations and hence is arbitrarily set equal to a large value such that $k_g >> k_d, k_c, k_1$.

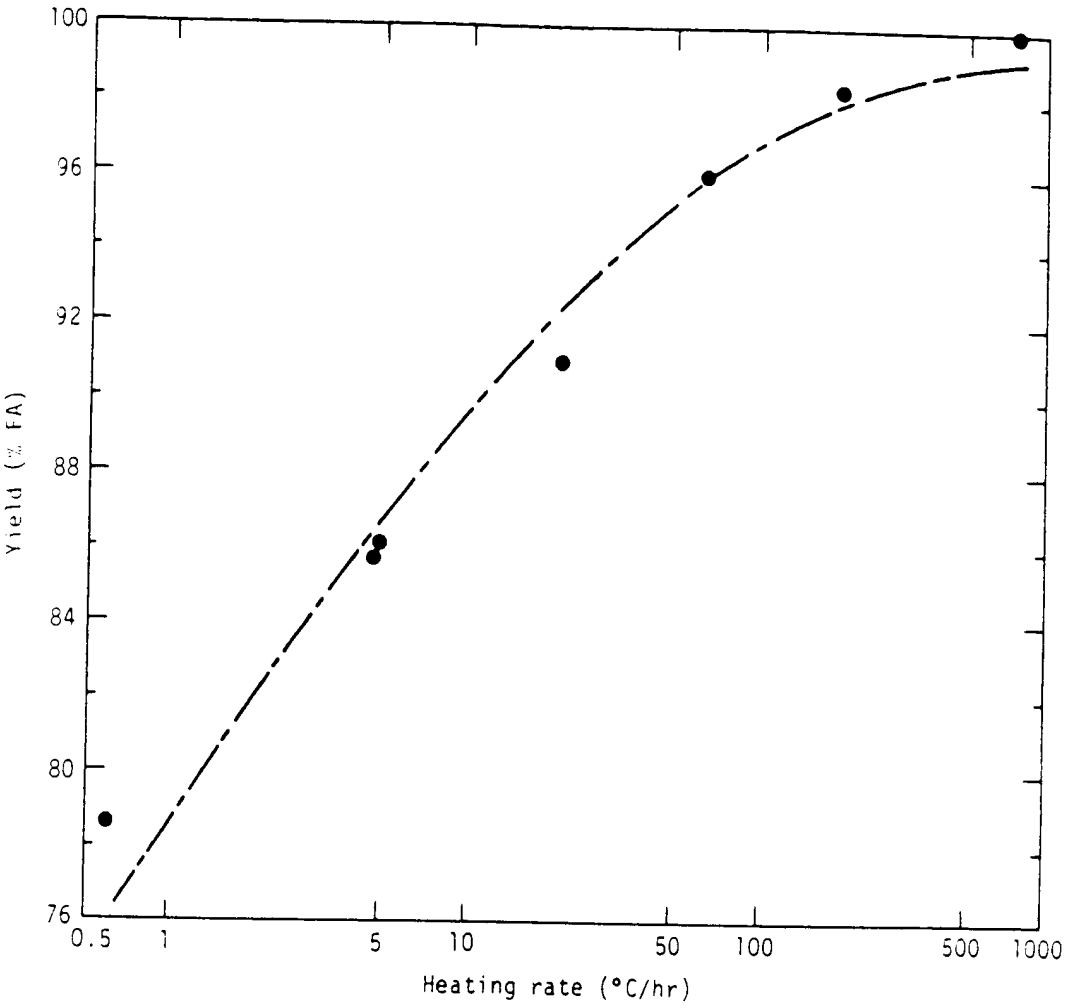

Fig. D1. Calculated (---) and observed (●) oil yield from powdered 22 gal/ton oil shale vs heating rate.

Unfortunately, no quantitative information is available for k_1, only the observation that k_1 α flow rate α heating rate; the proportionality constants are unknown. For a rate of coke production given by Eq. (2D) it was found that the value of k_1

$$k_1 = a \cdot \text{heating rate},$$

where

$$a \doteq 0.12\ ^{\circ}K^{-1}\ , \tag{3D}$$

gives excellent agreement with the observed yield for retorting of powders at a heating rate of 60°C/hr.

Using the above rate constants, the oil boiling point data in Appendix E and the mechanism shown in the main text [Eq. (2)], one can calculate the dependence of oil yield on heating rate for *powder* retorting experiments (Fig. D1). The calculations were carried out using a standard ordinary differential equation computer routine.[31]

APPENDIX E. BOILING POINT RANGE OF OIL PRODUCTS BY SIMULATED DISTILLATION

The distribution of products in the liquid and vapor phase was estimated via a gas chromatographic simulated distillation of a Fischer Assay oil (Fig. E1). In the numerical calculations it is assumed that the weight percent of the material completely in the gas phase (i.e., above its boiling point) is given by the expression (Fig. E1)

$$X(T) = 0.38 + (T - 325) \cdot 0.0035, \quad \text{for } T \geq 217^{\circ}C \tag{1E}$$

$$= 1.00, \quad \text{for } T > 500^{\circ}C\ .$$

The material not totally in the vapor phase is designated as oil[1] and is assumed to be at some equilibrium vapor-liquid distribution (see discussion in main text).

The rather poor agreement between Eq. (1E) and the distillation curve below 300°C (Fig. E1) has no effect on the calculations since retorting begins above 300°C.

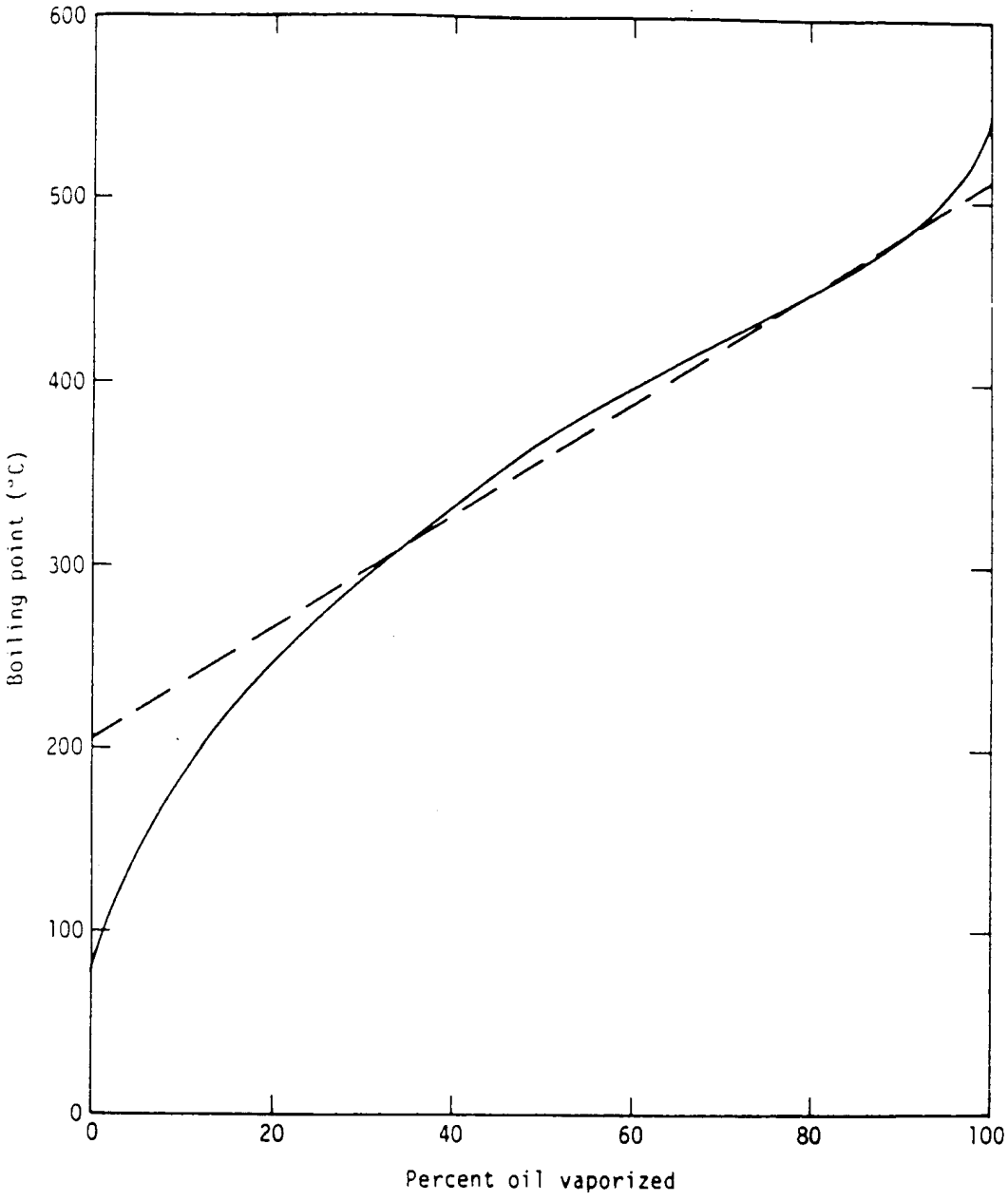

Fig. E1. Simulated distillation curve for Fischer Assay oil. Dashed line represents linear approximation of boiling point curve used in numerical calculations.

APPENDIX F. INTRAPARTICLE CONVECTIVE HEAT TRANSPORT

An accurate account of convective heat transport requires a detailed model description of fluid flow through the porous shale media. This not only greatly increases the complexity of the model but also necessitates the use of several free parameters, since little quantitative information is available on the properties (porosity and permeability) of the shale. In this appendix it is shown that for the case of a constant mass flux rate (similar to that encountered during retorting) the effect of convective heat transport is small compared to conduction and hence can be neglected.

From the data in Fig. 5 and Table 2 (main text) it can be shown that average mass flux rate ($\overline{\rho_g v_g}$) during retorting of a 17.2-cm diam 37 gal/ton shale block at a heating rate of 60°C/hr is approximately 8.7×10^{-4} kg/m^2 s. Assuming the average heat capacity of evolved product is 0.80 kcal/kg °C (that for n-decane), one can then determine the temperature distribution in the block with both convective and conductive heat transport. The method of solution is the same as that discussed in the main text. In the calculations the mass flux at a particular radial position in the block is assumed to begin with the onset of kerogen

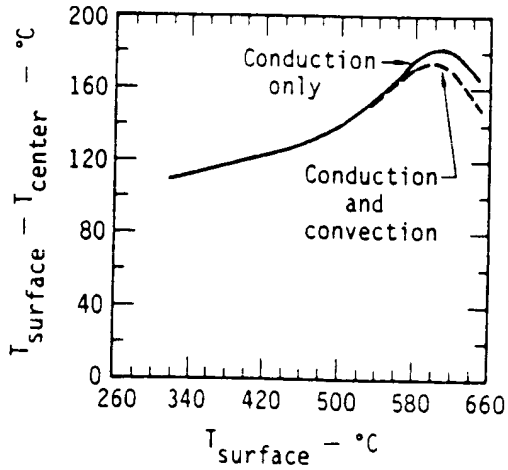

Fig. F1. Calculated temperature difference between block surface and center vs surface temperature. The dashed line is for heat transport by conduction and convection, whereas the solid line is for conduction only. The surface heating rate is 60°C/hr and the particle is 17.2 cm in diameter and 37 g/ton.

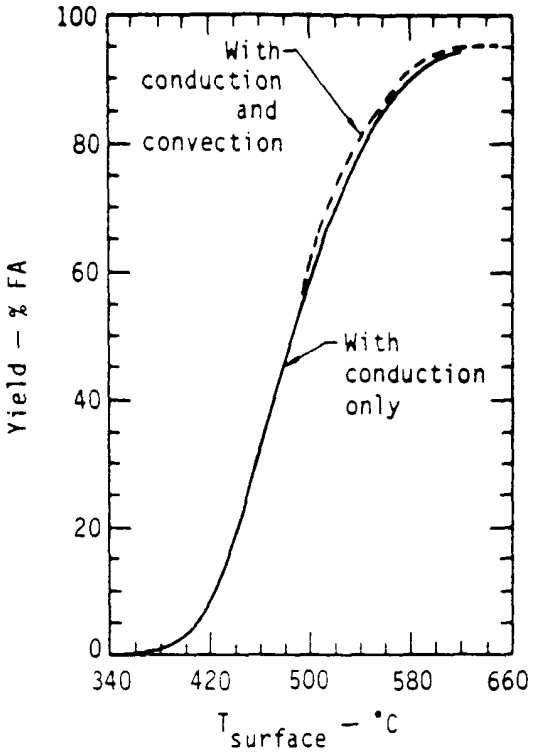

Fig. F2. Oil evolution vs block surface temperature calculated for the cases of heat transport by conduction only (-) and by conduction plus convective (---). The surface heating rate is 60°C/hr and the particle is 17.2-cm diam and 37 gal/ton.

decomposition and continue during the entire heating process.

The results of the above calculations are given in Fig. F1 and F2. Plotted is the temperature difference between the block surface and center (Fig. F1) and amount of oil evolved (Fig. F2) vs block surface temperature. Also shown are the results from calculations including only conduction. The results show that the convective effects are minor compared to conduction and consequently can be neglected.